NUMERICAL STUDY OF NATURAL CONVECTION IN HORIZONTAL ECCENTRIC ANNULUS

Waleed M. Abid
Mechanical engineering Dept.
University of Anbar.

Mohammed A. Ahmed
Mechanical engineering Dept.
University of Anbar.

ABSTRACT

This paper deals with a numerical investigation of natural convection of heat transfer in a horizontal eccentric annulus between a square outer enclosure and a heated circular inner cylinder.

The governing equations are expressed by the term of the stream function-vorticity with dimensionless temperature. The body fitted coordinate system (BFC) was used to stretch over the physical domain of the presented problem. The Poission's equation of stream function is solved by successive over relaxation (SOR) method, while time marching technique was the best choice to solve both vorticity and energy equation.

The results are presented for the streamlines and isotherms as well as the average Nusselt number at different eccentricities and angular positions. Comparison with previous theoretical results shows good agreement.

KEYWORDS: Numerical Study, Heat Transfer, Natural Convection, and Eccentricity.

INTRODUCTION

Natural Convection in the enclosed region formed between an isothermal heated body and its surrounding. Isothermal cooled enclosure is currently of some interest to designers of microelectronics equipment. In an effort to protect electronics from environmental contaminates such as dust or moisture, circuits are often housed in sealed enclosures, especially in outside plant applications. The ability to model natural convection heat transfer within these sealed enclosures would be of great benefit, providing quick and easy to use design tools for preliminary design tasks such as parametric studies and trade off analysis.

A large number of literatures were published in the past few decades. For concentric and eccentric cases in a horizontal annulus between two circular cylinders, the basic and fundamental configuration, the flow and thermal fields have been well studied.

In the first of two publications, Kuehn and Goldstein [1] presented the results of their experimental tests and numerical simulation of the horizontal annulus. Their experimental results included extensive documentation of temperature profiles and flow fields in the annular cavity, as well as average heat transfer results for air and water filled annuli. Numerical predictions of temperature and velocity profiles were also presented, and average effective conductivity were reported for (Pr= 0.7) for various aspect ratios and Rayliegh numbers. Simple correlations of the experimental results from a least-squares regression were also presented.

Kuehn and Goldstein [2] also developed a comprehensive model for heat transfer in concentric and eccentric circular annuli suitable for all values of the independent parameters (Do/Di), Pr and Ra. The formulation of this model included terms for pure conduction for

both concentric and eccentric geometric, as well as laminar and turbulent convection for the boundary layer limit. Results are

expressed in terms of the Nusselt number based on (Di) and the dimensionless effective conductivity ratio (Ke/K).

For concentric cases, Warrington and Powe [3] reported some experimental results of natural convection heat transfer between concentrically mounted bodies at low Rayleigh numbers. Liu et al. [4] studied the heat convection problem for the circular inner cylinder which was concentrically located inside a rectangular cylinder and only one aspect ratio was considered at two different Rayleigh numbers. The problem was solved by an operator splitting pseudo-time stepping finite element method.

Moukalled and Acharya [5] studied numerically natural convection heat transfer from a heated horizontal cylinder placed concentrically inside a square enclosure. The governing equations are solved in a body fitted coordinate system using a control volume based upon numerical procedure and their numerical data were validated by comparison with some experimental data and found in good agreement. For eccentric cases, Ekundayo et al. [6] studied experimentally the natural convection in horizontal annulus between a square outer cylinder and a circular inner cylinder.

Ghaddar [7] numerically studied the natural convection of heat transfer from uniformly heated of horizontal cylinder placed in a large air-filled rectangular enclosure. Sasaguchi et al. [8] numerically studied the effort of the position of a cooled cylinder in a rectangular cavity on the cooling process of water around the cylinder.

In the current study, the natural convection of heat transfer in a horizontal eccentric annulus between a square enclosure and heated circular inner cylinder is numerically studied using explicit method of finite difference based on the time marching technique. The effects of eccentricity and angular position of inner cylinder on the flow and thermal fields for the medium aspect ratio are studied in detail.

PROBLEM DESCRIPTION

The present paper studied the problem of natural convection in an eccentric annulus between a square outer enclosure and a circular inner cylinder. The inner cylinder is heated at a constant temperature (T_i), the outer cylinder is held at a colder temperature (T_o). A schematic diagram of the physical model and coordinate system is shown in Fig. 1.

The problem of interest involves convective heat transfer from an outer enclosure and an isothermal circular inner cylinder; heat is generated uniformly within the circular inner cylinder which is placed eccentrically with the cold square enclosure. There are no slip in the imposed boundary conditions as well as isothermal walls on both square outer enclosure and inner cylinder.

GOVERING EQUATIONS AND BOUNDARY CONDITIONS

For calculation purposes, it is often convenient to non-dimensionalize the governing equations and to introduce the characteristic dimensionless numbers. The Boussinesq approximation and the non-dimensional governing equations for the problem are written in the vorticity stream function formulation as: [9, 10]

$$\frac{\partial^2 Y}{\partial X^2} + \frac{\partial^2 Y}{\partial Y^2} = -w \qquad (1)$$

$$\frac{\partial w}{\partial t}+\frac{\partial Y}{\partial Y}\frac{\partial w}{\partial X}-\frac{\partial Y}{\partial X}\frac{\partial w}{\partial Y}=Pr\left(\frac{\partial^2 w}{\partial X^2}+\frac{\partial^2 w}{\partial Y^2}\right)-Pr\ Ra\ \frac{\partial q}{\partial X} \tag{2}$$

$$\frac{\partial q}{\partial t}+\frac{\partial Y}{\partial Y}\frac{\partial q}{\partial X}-\frac{\partial Y}{\partial X}\frac{\partial q}{\partial Y}=\left(\frac{\partial^2 q}{\partial X^2}+\frac{\partial^2 q}{\partial Y^2}\right) \tag{3}$$

where (Ψ) denotes stream function, (ω) represents vorticity, and (θ) is the dimensionless temperature. Prandtl number is defined as:

$$Pr=\frac{u}{a}=\frac{m C_p}{k} \tag{4}$$

and Rayleigh number is defined as:

$$Ra=\frac{C_p\ r_\circ\ g\ b\ L^3\ DT}{k\,u} \tag{5}$$

In the present study, the physical boundaries may not coincide with the mesh lines. When the explicit method is applied to this case, the physical boundary conditions can not be implemented in a straightforward way. To overcome this difficulty, the following transformation from the physical space to the computational space is required:

$$\left.\begin{aligned} x&=x(x,y)\\ h&=h(x,y)\end{aligned}\right\} \tag{6}$$

With this transformation, the governing Equations (1to 3) can be transformed to the following forms in the computational space:

$$\left(l'.\frac{\partial Y}{\partial z}+s'.\frac{\partial Y}{\partial h}+a'.\frac{\partial^2 Y}{\partial z^2}-2b'.\frac{\partial^2 Y}{\partial z\,\partial h}+g'.\frac{\partial^2 Y}{\partial h^2}\right)/J^2=-w \tag{7}$$

$$\frac{\partial w}{\partial t}+\frac{1}{J}\left(-\frac{\partial Y}{\partial z}.\frac{\partial w}{\partial h}+\frac{\partial Y}{\partial h}.\frac{\partial w}{\partial z}\right)=\frac{Pr}{J^2}\left(l'.\frac{\partial Y}{\partial z}+s'.\frac{\partial Y}{\partial h}+a'.\frac{\partial^2 Y}{\partial z^2}-2b'.\frac{\partial^2 Y}{\partial z\partial h}+g'.\frac{\partial^2 Y}{\partial h^2}\right)$$
$$-\left(\frac{Pr\ Ra}{J}\right)\left(\frac{\partial q}{\partial z}.\frac{\partial Y}{\partial h}+\frac{\partial q}{\partial h}.\frac{\partial Y}{\partial z}\right) \tag{8}$$

$$\frac{\partial q}{\partial t}+\left(-\frac{\partial Y}{\partial z}.\frac{\partial q}{\partial h}+\frac{\partial Y}{\partial h}.\frac{\partial q}{\partial z}\right)/J=\left(l'.\frac{\partial q}{\partial z}+s'.\frac{\partial q}{\partial h}+a'.\frac{\partial^2 q}{\partial z^2}-2b'.\frac{\partial^2 q}{\partial z\partial h}+g'.\frac{\partial^2 q}{\partial h^2}\right)/J^2 \quad (9)$$

where,

$$a'=x^2{}_h+y^2{}_h \quad , \quad s'=x_x\ x_h+y_x\ y_h \quad , \quad g'=x^2{}_x+y^2{}_x \quad , \quad J=x_x\ y_h-y_x\ x_h$$

$x_x\ ,x_h\ ,y_x\ ,y_h$ are respectively the abbreviations of $\frac{\partial x}{\partial x},\frac{\partial x}{\partial h},\frac{\partial y}{\partial x}$ and $\frac{\partial y}{\partial h}$.

The velocities (u, v) on both the inner isothermal cylinder and outer enclosure walls are zero. The stream function value on the enclosure wall is set zero in the present study. The boundary conditions can be written as:

$$y\big|_{h=0}=constant. \ , \ y\big|_{h=1}=0 \quad (10\ a)$$

$$q\big|_{h=0}=1 \quad , \quad q\big|_{h=1}=0 \quad (10\ b)$$

$$w\big|_{h=0,1}=\left.\frac{g'}{J}\frac{\partial^2 y}{\partial h^2}\right|_{h=0,1} \quad (10\ c)$$

NUMERICAL METHOD

The two equations of vorticity transport and energy are solved by explicit method of finite difference based on the time marching technique. The time marching technique is used for solving the unsteady governing equations to obtain the steady velocity and temperature distributions. The governing equations are based on studying the time development of the velocity and thermal fields until reaching steady conditions. These equations are

$$w^{\,n+1}_{(i,j)}=w^{\,n}_{(i,j)}+\Delta t\left[\frac{1}{J_{(i,j)}}\left(\frac{\Psi_{(i+1,j)}-\Psi_{(i-1,j)}}{2.\Delta x}.\frac{w^{\,n}_{(i,j+1)}-w^{\,n}_{(i,j-1)}}{2.\Delta h}-\frac{\Psi_{(i,j+1)}-\Psi_{(i,j-1)}}{2.\Delta h}.\right.\right.$$
$$\left.\frac{w^{\,n}_{(i+1,j)}-w^{\,n}_{(i-1,j)}}{2.\Delta x}\right)+\frac{\Pr}{J^{\,2}_{(i,j)}}\left(l'_{(i,j)}.\frac{w^{\,n}_{(i+1,j)}-w^{\,n}_{)i-1,j)}}{2.\Delta x}.s'_{(i,j)}.\frac{w^{\,n}_{(i,j+1)}-w^{\,n}_{(i,j-1)}}{2.\Delta h}\right.$$
$$+a'_{(i,j)}.\frac{w^{n}_{(i+1,j)}-2.w^{n}_{(i,j)}+w^{n}_{(i-1,j)}}{\Delta x^{\,2}}-2.b'_{(i,j)}.\frac{w^{n}_{(i+1,j+1)}-w^{n}_{(i+1,j-1)}-w^{n}_{(i-1,j+1)}+w^{n}_{(i-1,j-1)}}{4.\Delta x.\Delta h}$$

$$\left.+g'_{(i,j)}.\frac{w^{\,n}_{(i,j+1)}-2.w^{\,n}_{(i,j)}+w^{\,n}_{(i,j-1)}}{\Delta h^{\,2}}\right)-\frac{\Pr\ Ra}{J_{(i,j)}}\left(\frac{q^{\,n}{}_{(i+1,j)}-q^{\,n}{}_{(i-1,j)}}{2\Delta x}.\frac{Y_{(i,j+1)}-Y_{(i,j-1)}}{2\Delta h}\right.$$
$$\left.+\frac{q^{\,n}{}_{(i,j+1)}-q^{\,n}{}_{(i,j-1)}}{2\Delta h}.\frac{Y_{(i+1,j)}-Y_{(i-1,j)}}{2\Delta x}\right) \quad (11)$$

$$q^{n+1}_{(i,j)} = q^{n}_{(i,j)} + \Delta t \left[\frac{1}{J_{(i,j)}} \left(\frac{\Psi_{(i+1,j)} - \Psi_{(i-1,j)}}{2.\Delta x} \cdot \frac{q^{n}_{(i,j+1)} - q^{n}_{(i,j-1)}}{2.\Delta h} - \frac{\Psi_{(i,j+1)} - \Psi_{(i,j-1)}}{2.\Delta h} \cdot \frac{q^{n}_{(i+1,j)} - q^{n}_{(i-1,j)}}{2.\Delta x} \right) + \frac{1}{J^{2}_{(i,j)}} \left(l'_{(i,j)} \cdot \frac{q^{n}_{(i+1,j)} - q^{n}_{(i-1,j)}}{2.\Delta x} \cdot s'_{(i,j)} \cdot \frac{q^{n}_{(i,j+1)} - q^{n}_{(i,j-1)}}{2.\Delta h} \cdot + a'_{(i,j)} \cdot \frac{q^{n}_{(i+1,j)} - 2.q^{n}_{(i,j)} + q^{n}_{(i-1,j)}}{\Delta x^{2}} - 2.b'_{(i,j)} \cdot \frac{q^{n}_{(i+1,j+1)} - q^{n}_{(i+1,j-1)} - q^{n}_{(i-1,j+1)} + q^{n}_{(i-1,j-1)}}{4.\Delta x.\Delta h} + g'_{(i,j)} \cdot \frac{w^{n}_{(i,j+1)} - 2.w^{n}_{(i,j)} + w^{n}_{(i,j-1)}}{\Delta h^{2}} \right) \right] \quad (12)$$

But, the stream function equation are solved by relaxation method as follows

$$l'_{(i,j)} \cdot \frac{\Psi_{(i+1,j)} - \Psi_{(i-1,j)}}{2.\Delta x} + s'_{(i,j)} \cdot \frac{\Psi_{(i,j+1)} - \Psi_{(i,j-1)}}{2.\Delta h} + a'_{(i,j)} \cdot \frac{\Psi_{(i+1,j)} - 2\Psi_{(i,j)} + \Psi_{(i-1,j)}}{\Delta x^{2}} + g'_{(i,j)} \cdot \frac{\Psi_{(i,j+1)} - 2\Psi_{(i,j)} + \Psi_{(i,j-1)}}{\Delta h^{2}} - 2b'_{(i,j)} \cdot \frac{1}{2\Delta x} \left(\frac{\Psi_{(i+1,j+1)} - \Psi_{(i+1,j-1)}}{2.\Delta x} - \frac{\Psi_{(i-1,j+1)} - \Psi_{(i-1,j-1)}}{2.\Delta h} \right) + J^{2}_{(i,j)} \cdot w_{(i,j)} = Error \approx 0 \quad (13)$$

Theoretically the accuracy of solution depends on small grid size and the time step been used to expect, that the solutions will be reasonably accurate. A uniform grid 99x20 in the transformed computational domain was considered suitable for covering the computational domain. The dimensionless time step used in the present study was 10^{-6}.

CALCULATION OF NUSSELT NUMBER

When the solution convergence criterion is reached, the local and mean Nusselt number on the inner cylinder walls are calculated. From the balance of heat flux at the surface, the Nusselt number for inner cylinder can be obtained as:

$$Nu = -\frac{\partial q}{\partial n}$$

(14) Now, Eq. (14) is transformed into general coordinate (ζ,η) as follows

$$Nu = \frac{1}{J\sqrt{g'}} \left[g' q_h - b' q_x \right] \quad (15)$$

Since the temperature along the wall cylinder (w) is constant, $\frac{\partial q}{\partial x} = 0$, Eq. (15) becomes

$$Nu = \frac{g'}{J\sqrt{g'}} q_h \quad (16)$$

The Nusselt number in Eq. (16) is the local Nusselt number. To find the average Nusselt number, the local Nusselt number should be integrated by using numerical integration.

RESULTS AND DISCUSSION

The numerical solution of the present problem is obtained for different eccentricities and angular positions of the cylinder at Rayleigh numbers of 10^4, 10^5, and 10^6 while Prandtl number is fixed at 0.71.

In this study, the results of Moukalled and Acharya [5] are used to validate the present numerical results. The average Nusselt number between the present work and the work of

Moukalled and Acharya [5] are compared in Fig. 2 for Rayleigh number of (10^4), Prandtl number (0.71) and aspect ratios of (1.67, 2.5 and 5). The present results are deviated from that Moukalled and Acharya [5] due to the different ways of non-dimensionalization. From Fig. 2, it can be seen that the present results agree well with those of Moukalled and Acharya [5].

Fig. 3 shows the average Nusselt number versus the aspect ratios at Rayleigh numbers of (10^4, 10^5 and 10^6). The computation results of the average Nusselt number shown in Fig. 4. The streamlines and isotherms are shown in Fig. (5) to Fig. (9) for different angular positions.

For $\lambda = 0°$ as shown in Fig. 5, the flow and thermal fields are symmetric. The flow fields show explicitly that the two centers of the two symmetric eddies on the left hand side and right hand side move closer with eccentricity. This is because of the great space available for circulation to occur when the eccentricity increases, and the two eddies increase their size towards the centre of the square outer enclosure. The stagnant area under the inner cylinder decreases with increase of eccentricity but still exists at the two bottom corners of the square enclosure. A large plume exists in the large gap above the inner cylinder, which creates a thinner thermal boundary layer on top of the square enclosure.

For $\lambda = 180°$ as shown in Fig. 6, the flow and thermal fields are symmetric. The maximum value of stream function decreases with eccentricity considerably, and the stagnant area increases with the increase of eccentricity.

For $\lambda = 45°$ as shown in Fig. 7, the eddy on the left hand side in the flow expands in size due to the increasing space with the center of the eddy moving downwards. The eddy on the right hand side retains its size but shifts above the inner cylinder. The increasing eccentricity allows larger space for the eddy on the right hand side, but the increasing eddy on the left-hand side limits the space for the eddy on the right hand side. The plume above the top of the inner cylinder shifts from the vertical line to the left. The stagnant area decreases with eccentricity.

For $\lambda = 90°$ as shown in Fig. 8, the eddy on the left-hand side in the flow expands in size due to the increasing space. The eddy on the right-hand side separates into two small eddies, above and below the inner cylinder respectively with increasing of eccentricity. The maximum values of stream function are about the same level at different eccentricities, where the inner cylinder is very close to the wall of the outer enclosure.

For $\lambda = 135°$ as, shown in Fig. 9, the eddy on the right-hand side finally separates into two vorticies with eccentricity due to the reduced space. The plume above the top of the inner cylinder increases from one to two due to the decreased space with eccentricity. The stagnant area under the inner cylinder increases with eccentricity.

CONCLUSIONS

The natural convection between arbitrary eccentric cylinder for Ra= 10^4 and aspect ratio of rr=2.6 is systematically analyzed, including the effects of outer enclosure position on average Nusselt number, flow and thermal fields. It was found that global circulation, flow separation and the top space between the square outer enclosure and the circular inner cylinder have significant effects on the plume inclination.

REFERENCES

[1] T.H. Kuehn, R.J. Goldstein, An experimental and theoretical study of natural convection in the annulus between horizontal concentric cylinders, J. Fluid Mech. Vol.74 (1976).

[2] T.H. Kuehn, R.J. Goldstein, An experimental study of natural convection in the concentric and eccentric horizontal cylindrical annuli, ASME J. Heat Transfer. Vol.100 (1978).

[3] R.O. Warrington, R.E. Powe, The transfer of heat by natural convection between bodies and their enclosures, Int. J. Heat Mass Transfer. Vol. 2 (1985).

[4] Y. Liu, N. Phan, R. Kemp, Coupled conduction-convection problem for a cylinder in an enclosure, Comput. Mech. Vol. 18 (1996).
[5] F. Moukalled, S. Acharya, Natural convection in the annulus between concentric horizontal circular and square cylinders, J. Thermophys. Heat Transfer. Vol. 10 (1996).
[6] C.O. Ekundayo, S.D. Probert, M. Newborough, Heat transfer from a horizontal cylinder in a rectangular enclosure, Appl. Energy. Vol. 61 (1998).
[7] N.K. Ghaddar, Natural convection heat transfer between a uniformly heated cylindrical element and rectangular enclosure, Int. J. Heat Mass Transfer. Vol. 35 (1992).
[8] K. Sasaguchi, K. Kuwabara, K. Kusano, Transient cooling of water around a cylinder in a rectangular cavity – a numerical analysis of the effect of the position of the cylinder, Int. J. Heat Mass Transfer. Vol.41 (1998).
[9] A. Bejan, Heat Transfer, Wiley, New York, (1993).
[10] L. Crawford, R. Lemlich, Natural convection in horizontal concentric cylindrical annuli, Industrial and Engineering Chemistry Fundamentals, vol. 1, (1962).

NOMENCLATURE

Cp	specific heat at constant pressure (kJ/kg ºC).
e	eccentricity (m).
g	gravitational acceleration (m/s^2).
h	heat transfer coefficient (w/m^{2}ºC).
k	thermal conductivity (w/mºC).
L	side length of the square outer enclosure (m).
Nu	Nusselt number.
Pr	Prandtl number.
r_i	radius of inner cylinder (m).
r_o	distance from the outer square enclosure to the origin (m).
Ra	Rayleigh number.
rr	aspect ratio (L/2ri)
x,y	Coordinates
u,v	velocity components along x and y directions, respectively (m/s).

Greek symbols:

α	thermal diffusivity (m^2/s).
β	thermal expansion coefficient (1/K).
θ	non-dimensional temperature (ºC).
ξ, η	transformed coordinates.
Ψ	stream function.
ω	vorticity
ρ_o	reference density (kg/m^3).
μ	viscosity (kg/ms).
ν	kinematic Viscosity (m^2/s).
τ	dimensionless of time.
λ	angular position of outer enclosure.

Subscripts:

i	inner cylinder wall.
o	outer square enclosure wall.

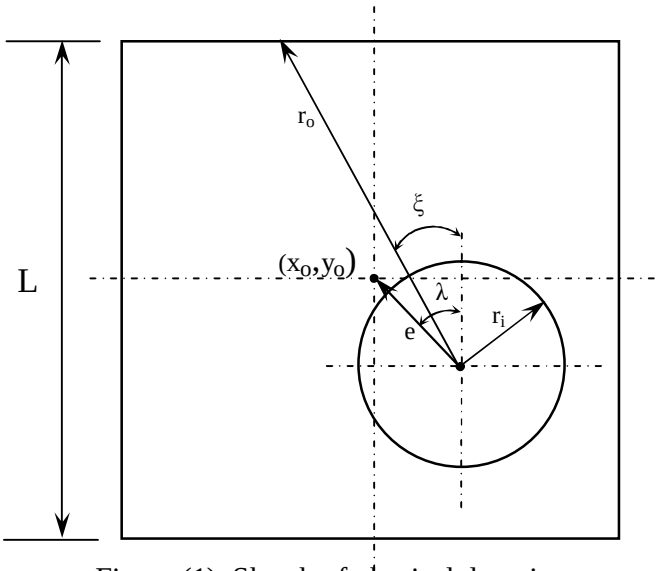

Figure (1): Sketch of physical domain.

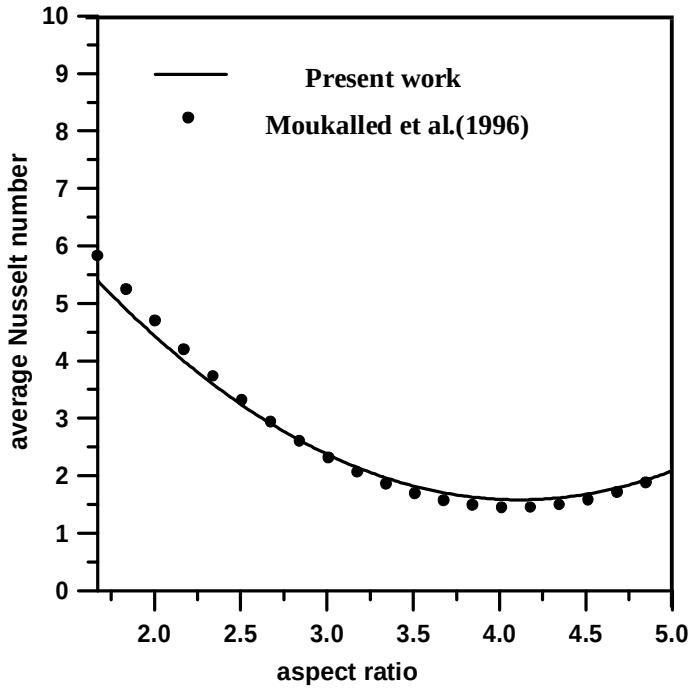

Figure (2): average Nusselt number versus aspect ratio (Ra =10^4, Pr =0.71)

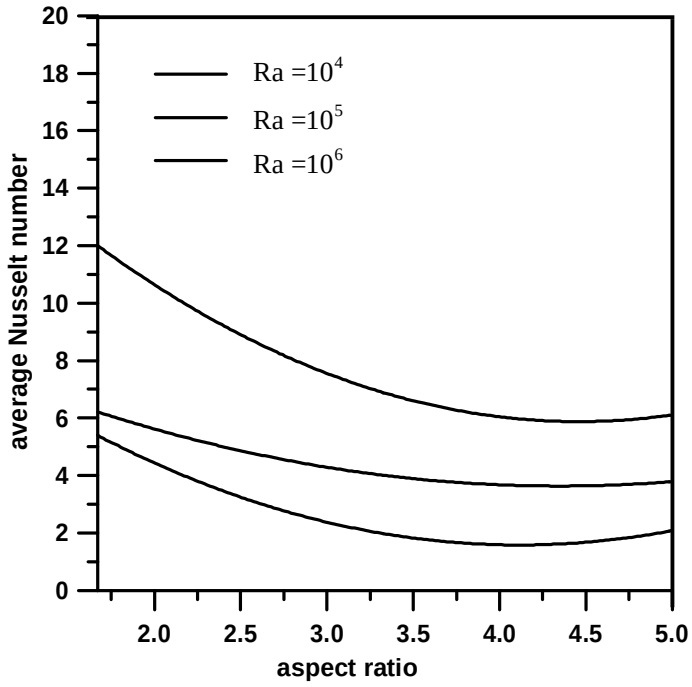

Figure (3): average Nusselt number versus aspect ratio.

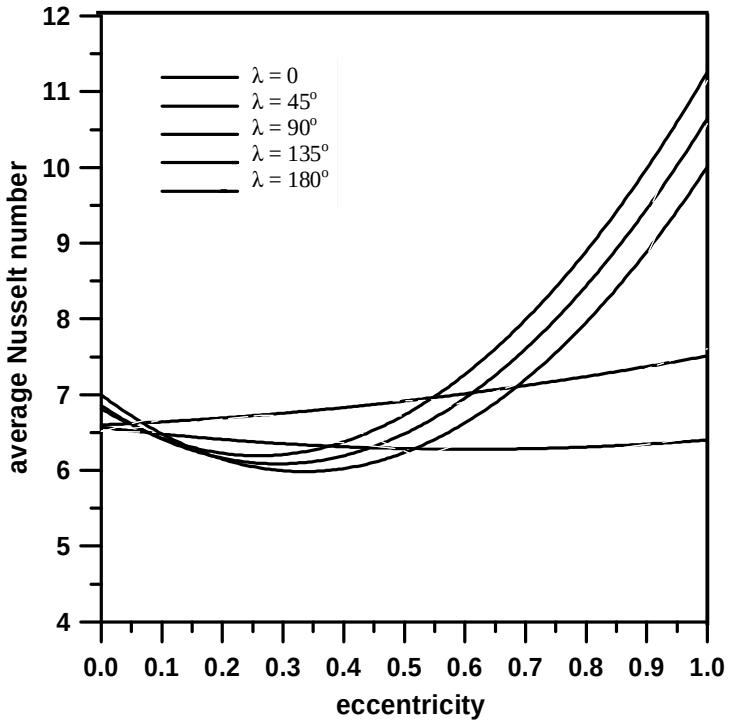

Figure (4): average Nusselt number versus eccentricity at rr=2.6, Ra =10^4 and Pr =0.71.

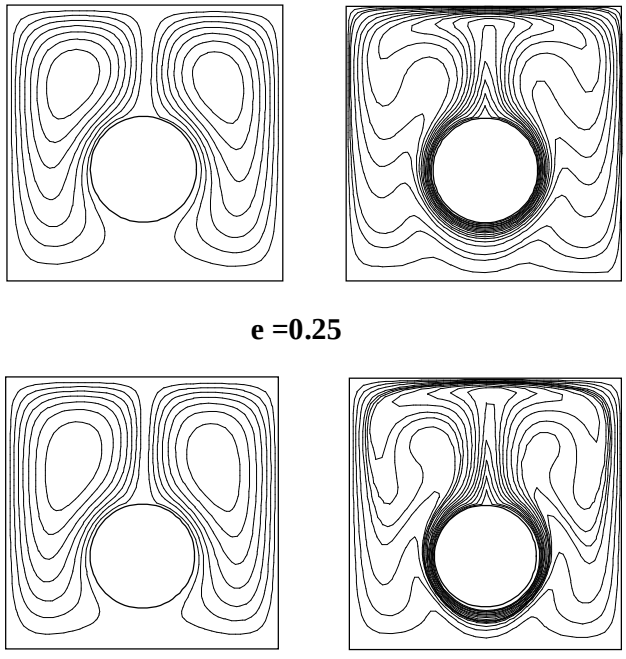

Figure (5): Streamlines and isotherms for Ra=10^4, Pr=0.71, rr=2.6, λ=0^o

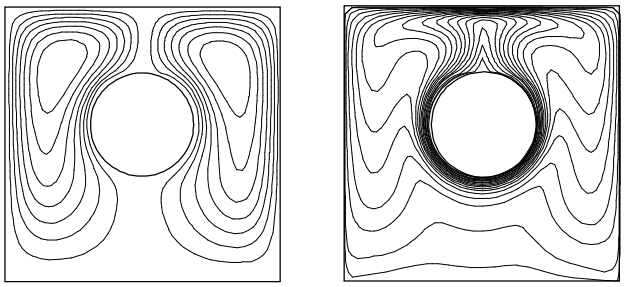

e =0.25

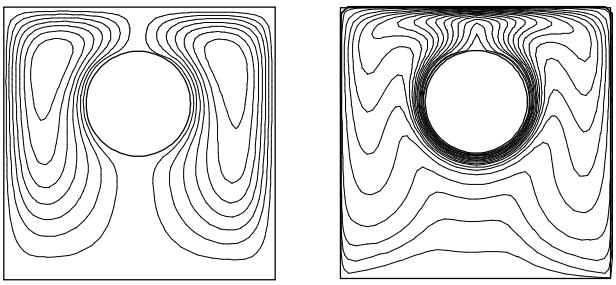

e =0.5

Figure (6): Streamlines and isotherms for $Ra=10^4$, Pr=0.71, rr=2.6, $\lambda=180^o$.

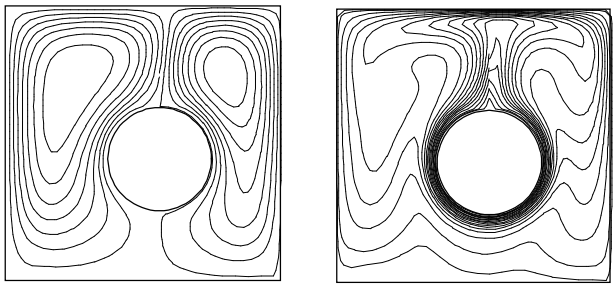

e =0.25

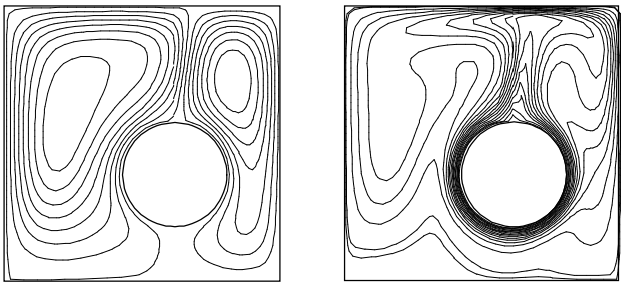

e =0.5

Figure (7): Streamlines and isotherms for $Ra=10^4$, Pr=0.71, rr=2.6, $\lambda=45^o$.

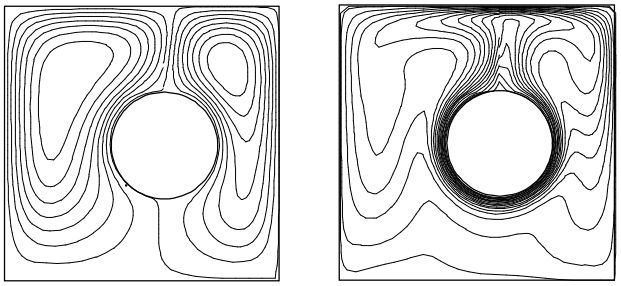

e =0.25

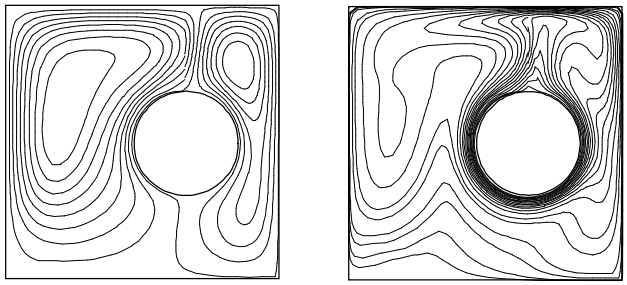

e =0.5

Figure (8): Streamlines and isotherms for $Ra=10^4$, Pr=0.71, rr=2.6, $\lambda=90^o$.

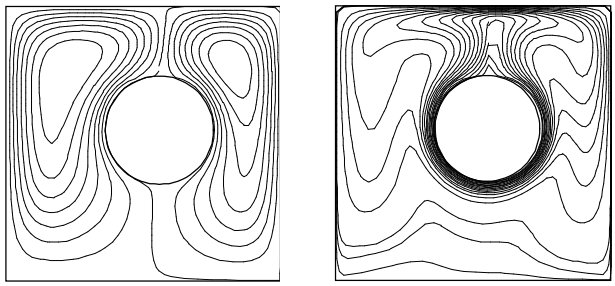

e =0.25

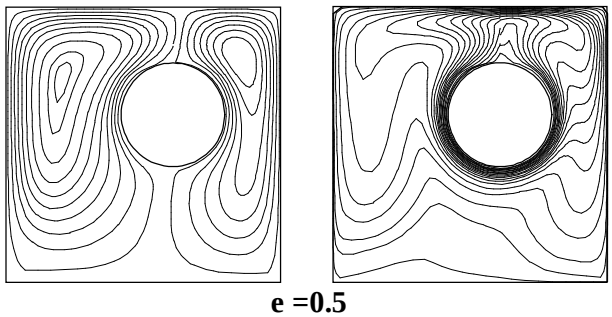

e =0.5

Fig. (9) Streamlines and isotherms for $Ra=10^4$, Pr=0.71, rr=2.6, $\lambda=135^o$.

دراسة عددية للحمل الحر من أنبوب حلقي أفقي لامركزي

وليد محمد عبد
قسم الهندسة الميكانيكية
جامعة الانبار

محمد عبد احمد
قسم الهندسة الميكانيكية
جامعة الانبار

الخـــلاصـــة

تضمن هذا البحث دراسة عددية لانتقال الحرارة بالحمل الحر لأنبوب حلقي أفقي لامركزي. المعادلات الحاكمة وضعت بصيغة دالة الانسياب-دوامية ودرجة حرارة اللابعدية. استخدم نظام مطابقة إحداثيات الجسم (BFC) ليغطي المجال الفيزيائي للمسألة الحالية. معادلة بويسن لدالة الانسياب حلـــت بواســـطة طريقة الإرخاء المتعاقب (SOR) ، بينما أثبتت تقنية الارتحال الزمني انها الاختيار الأفضل لحل كـــل من معادلة الدوامية والطاقة.

مثلت النتائج لخطوط الانسياب ودرجة الحرارة بالإضافة إلى متوسط عدد نسلت عند مواقع لامركزية وزاوية مختلفة. أوضحت المقارنة مع نتائج نظرية سابقة توافق جيد بينهما.